GMR
The Original

ASSEMBLY OF MULTIFUNCTIONAL STARCH/PVA ELECTROSPUN NANOSCAFFOLDS INCORPORATED WITH ULTRASONIC-ASSISTED BIOGENIC SYNTHESIS OF CuO NANOPARTICLES FROM MARINE MACROALGAE (*DICTYOTA* SP.) EXTRACT: PHYSICOCHEMICAL CHARACTERIZATION AND ANTIDIABETIC EVALUATION

Deepthi Jeya Senthil Kumar[1], Palchuri Sneha Ananya[2], Balaguru Natarajan[2], Alagendran Subbarayalu[3]*

[1]Saveetha Medical College & Hospital (SMCH), Saveetha Institute of Medical and Technical Sciences (SIMATS), Thandalam, Chennai, Tamil Nadu 602105, India. deepthisenthilkumar04@gmail.com
[2]Department of Dermatology, Saveetha Medical College and Hospital, Saveetha Institute of Medical And Technical Sciences (SIMATS), Thandalam, Chennai-602105, Tamil Nadu, India. Email: sneha2000reddy@gmail.com; bala1guru@gmail.com
[3]Clinical Neuroscience and Phytomedicine Laboratory, Department of Research, Saveetha College of Nursing (SCON), Saveetha Institute of Medical and Technical Sciences (SIMATS), Chennai 602105, Tamil Nadu, India. Email: proteinblg@gmail.com; alagendrans.scon@saveetha.com. ORCID: https://orcid.org/0009-0009-0749-7180.
*Correspondence: proteinblg@gmail.com; alagendrans.scon@saveetha.com (A.S.)

ABSTRACT
This study explores the green synthesis of copper oxide nanoparticles (CuO NPs) using *Dictyota* algal extract and their incorporation into starch/polyvinyl alcohol (PVA) nanofiber scaffolds for enhanced antidiabetic activity. CuO NPs were synthesized via an eco-friendly approach, where algal bioactives acted as reducing and stabilizing agents. The nanoparticles were characterized using UV-Vis spectroscopy, FTIR, XRD, SEM, and DLS, confirming successful formation and high stability (zeta potential > ±30 mV). The starch/PVA/CuO-NPs nanoscaffolds were fabricated via electrospinning, exhibiting uniform fiber morphology (SEM) and improved thermal stability (TGA). *In vitro* antidiabetic evaluation demonstrated significant α-amylase and α-glucosidase inhibition, with nanoscaffolds showing the highest efficacy (IC_{50} = 52.32 µg/mL and 48.75 µg/mL, respectively) compared to algal extract and bare CuO NPs. The enhanced inhibitory effects were attributed to the synergistic interaction between CuO NPs and the polymeric matrix, facilitating controlled bioactive release. These findings highlight the potential of marine algae-mediated nanoscaffolds as a sustainable, biocompatible alternative for diabetes management. Further *in vivo* studies are recommended to assess therapeutic potential and biosafety.

KEYWORDS: *Dictyota sp.*, Green synthesis, CuO nanoparticles, Starch/PVA/CuO-NPs nanoscaffolds, Antidiabetic activity.

1. INTRODUCTION

Diabetes mellitus is a multifaceted chronic metabolic disorder characterized primarily by elevated blood glucose levels, resulting from impaired insulin secretion, reduced insulin action, or a combination of both [1]. This dysregulation leads to persistent hyperglycemia, which is associated with serious complications including cardiovascular disease, neuropathy, nephropathy, and retinopathy [2]. Globally, the incidence of diabetes is rising at an unprecedented pace, with recent statistics estimating that over 700 million people worldwide will be living with the condition by 2045 if current trends continue [3]. Among the different types of diabetes, type 2 diabetes mellitus (T2DM) accounts for approximately 90% of cases and is strongly linked to lifestyle factors such as poor diet, obesity, and physical inactivity [4].

Management of T2DM typically involves a combination of lifestyle modification strategies and pharmacological treatments aimed at maintaining glycemic control and preventing complications [5]. One of the therapeutic approaches involves inhibiting carbohydrate-digesting enzymes like α-amylase and α-glucosidase, which are responsible for breaking down complex carbohydrates into glucose [6]. Drugs such as acarbose and miglitol function by inhibiting these enzymes, thus reducing postprandial blood glucose spikes [7]. However, despite their effectiveness, these synthetic drugs often cause undesirable side effects including gastrointestinal discomfort, diarrhea, and in some cases, hepatotoxicity [8]. Furthermore, the high cost and long-term safety concerns

associated with these agents have driven research toward safer, more cost-effective, and sustainable alternatives [9].

Natural products, particularly those derived from marine ecosystems, have gained significant interest due to their vast chemical diversity and potent bioactivities [10]. Marine macroalgae, such as species belonging to the genus *Dictyota*, are known to contain a rich reservoir of bioactive constituents including polyphenols, flavonoids, sulfated polysaccharides, and terpenoids [11]. These compounds exhibit multiple biological properties, including enzyme inhibitory, antioxidant, anti-inflammatory, and antidiabetic effects, making them attractive candidates for therapeutic development [12]. However, the clinical utility of these natural extracts is often hampered by poor bioavailability and stability, necessitating novel delivery systems to harness their full therapeutic potential [13].

Nanotechnology offers promising solutions to these limitations by enabling the fabrication of nanoscale delivery platforms that improve the solubility, stability, and targeted release of bioactive molecules [14]. Among various nanomaterials, copper oxide nanoparticles (CuO NPs) have emerged as versatile agents with catalytic, antimicrobial, and antidiabetic properties [15]. CuO NPs have shown promising enzyme inhibitory activity, making them potential candidates for managing diabetes [15]. Traditional chemical methods for synthesizing CuO NPs, however, commonly rely on hazardous chemicals and harsh conditions, which raise concerns about environmental impact and biocompatibility [16]. To overcome these challenges, green synthesis approaches that utilize biological extracts—such as those from plants or algae—serve as eco-friendly alternatives [17]. These biological extracts act both as reducing agents, converting copper ions to nanoparticles, and as stabilizers, preventing aggregation [18]. This green synthesis method not only reduces environmental hazards but also enhances the biomedical applicability of the nanoparticles [16].

Complementing nanoparticle synthesis, electrospun nanofiber scaffolds fabricated from biocompatible polymers like starch and polyvinyl alcohol (PVA) represent innovative platforms for sustained drug delivery and tissue engineering applications [19]. These nanofibrous matrices possess high surface area-to-volume ratios, porosity, and mechanical strength, all of which contribute to their ability to encapsulate and release therapeutic agents in a controlled manner [20]. The incorporation of CuO NPs into such polymeric scaffolds is anticipated to synergistically enhance the antidiabetic efficacy by combining the bioactivity of the nanoparticles with the structural and functional advantages of the nanofibers [21]. Despite these potential benefits, research investigating the integrated effects of marine algae-mediated CuO NPs within biopolymer nanoscaffolds for diabetes treatment remains scarce.

The present study seeks to address this gap by (1) utilizing *Dictyota* extract to green-synthesize CuO NPs, (2) developing starch/PVA-based electrospun nanofiber scaffolds embedded with the biosynthesized CuO NPs, and (3) evaluating the antidiabetic potential of these composites through *in vitro* inhibition assays targeting α-amylase and α-glucosidase enzymes. Comprehensive physicochemical characterizations including UV-Visible spectroscopy, Fourier transform infrared spectroscopy (FTIR), X-ray diffraction (XRD), scanning electron microscopy (SEM), dynamic light scattering (DLS), and thermogravimetric analysis (TGA) were employed to confirm nanoparticle formation, assess scaffold morphology, and determine thermal stability. The findings aim to contribute to the growing field of nanobiotechnology by providing a novel, biocompatible nanotherapeutic approach that bridges the advantages of marine natural products with advanced materials engineering, potentially offering safer and more effective solutions for diabetes management.

2. MATERIALS AND METHODS

2.1 Chemicals and reagents

The brown marine macroalga *Dictyota* was harvested from the coastal waters near Rameswaram, Tamil Nadu, India, and utilized as a natural source for synthesizing CuO NPs through an eco-friendly green synthesis approach. Copper (II) sulfate pentahydrate ($CuSO_4 \cdot 5H_2O$), of analytical grade, served as the metal precursor for nanoparticle formation. PVA with a molecular weight of ~115,000 g/mol and starch were selected as scaffold-forming agents due to their excellent biocompatibility. The electrospinning procedure was carried out using the HOLMARC HO-NFES-040 apparatus. All solvents and reagents, obtained from Merck and Sigma-Aldrich, were of high analytical purity to ensure experimental reliability. Characterization of the synthesized materials was conducted using UV–Visible spectroscopy, FTIR, XRD, SEM, DLS, zeta potential measurements, and TGA. The biological potential, specifically the antidiabetic activity, was evaluated following standardized *in vitro* protocols.

2.2 Collection and processing of marine algae

Fresh *Dictyota* samples were hand-collected from the intertidal zones of the Rameswaram shoreline. After collection, the specimens were transported under chilled conditions to maintain bioactivity. The algal biomass was initially rinsed thoroughly under running tap water to eliminate adhering sand and epiphytes, followed by

successive washes with distilled water to remove any remaining salt and particulate matter. Cleaned samples, approximately 100 grams in weight, were chopped into small segments and air-dried at room temperature over a two-week period. The dried material was pulverized into a fine powder using a mechanical grinder and stored in airtight containers for extraction and nanoparticle synthesis.

2.3 Extraction of bioactives via ultrasonic treatment

To obtain bioactive compounds, 2 grams of powdered algae were dispersed in 50 mL of Milli-Q water in a 100 mL borosilicate beaker. The suspension was treated in a LABQUEST ultrasonic cleaner (Borosil; Serial No. 941032329018) at 60°C for 45 minutes. This ultrasonic-assisted extraction method promoted disruption of cell walls and facilitated the release of intracellular metabolites. The extract was filtered through sterile Whatman No. 1 filter paper to eliminate solid residues. The resulting filtrate was stored at 10°C for further use. A portion of the extract was freeze-dried to enhance shelf-life and yield a powder suitable for nanoparticle synthesis [22, 23].

2.4 Green synthesis of CuO NPs

CuO NPs were synthesized by mixing 50 mL of 0.1 M $CuSO_4 \cdot 5H_2O$ solution with 10 mL of the *Dictyota* extract (10 mg/mL concentration). The mixture was maintained at a 5:1 volume ratio and stirred continuously at 650 rpm on a temperature-controlled magnetic stirrer set at 60°C for 2 hours. The transformation from deep blue to a bluish-green hue indicated nanoparticle formation, likely facilitated by phytochemicals acting as reducing agents. The product was washed thrice with double-distilled water to remove unreacted biological components and salts. The purified CuO NPs were freeze-dried for 48 hours to obtain a stable powder for further processing and analysis [24].

2.5 Fabrication of starch/PVA/CuO nanofiber scaffolds

A 15% (w/w) aqueous PVA solution was prepared by dissolving PVA in Milli-Q water under magnetic stirring at 50°C. Once the polymer was fully dissolved, 100 mg of starch and 100 mg of the synthesized CuO NPs were added. The solution was stirred for 2.5 hours at 50°C to ensure homogeneity. The resulting mixture was loaded into a syringe equipped with a 0.84 mm stainless steel nozzle. Electrospinning was conducted using a HOLMARC HO-NFES-040 setup with the following parameters: applied voltage of 11.5 kV, nozzle-to-collector distance of 12.3 cm, and a feed rate of 0.4 mL/h. The process was continued for 6–8 hours at ambient conditions to form continuous nanofibrous mats, which were subsequently stored in a desiccator for characterization and bioanalysis [25-27].

2.6 Physicochemical characterization

2.6.1 UV–Vis Spectroscopy

Optical characterization of the algal extract, CuO NPs, and composite scaffolds was carried out using a VIS SPEC V-730 UV–Vis spectrophotometer. Samples were scanned in the 200–800 nm wavelength range with deionized water as a reference. Distinct absorption bands around 270–300 nm confirmed surface plasmon resonance (SPR), indicative of CuO NP formation and interaction within the scaffold [28].

2.6.2 FTIR analysis

FTIR analysis was performed on the algal extract, CuO NPs, and nanofiber scaffolds using a PerkinElmer Spectrum Two spectrometer in ATR mode. Spectra were recorded between 4000–400 cm^{-1} at 4 cm^{-1} resolution over 64 scans. Key vibrational peaks corresponding to functional groups like hydroxyl, carbonyl, amide, and metal–oxygen bonds confirmed successful nanoparticle formation and bioactive conjugation [29].

2.6.3 XRD analysis

Crystallinity and phase structure were analyzed using a Bruker D8 Advance diffractometer with CuKα radiation (λ = 1.5406 Å), operated at 40 kV and 40 mA. The scans covered 2θ angles from 5° to 90° with a step size of 0.029649°. Characteristic peaks of monoclinic CuO validated nanoparticle formation, while broadening of peaks in the scaffold confirmed polymer embedding [30].

2.6.4 SEM analysis

SEM imaging was conducted on the nanofiber scaffolds using a JEOL JSM-IT800 NANO microscope after sputter-coating with gold. Micrographs revealed detailed fiber architecture, diameter uniformity, and nanoparticle distribution, affirming effective electrospinning and CuO incorporation [31].

2.6.5 TGA

Thermal stability was evaluated using a PerkinElmer TGA 8000 analyzer. Approximately 5 mg of sample was heated from room temperature to 550°C at a rate of 15°C/min under nitrogen. The thermograms indicated moisture evaporation, polymer degradation, and residual mass due to CuO NPs, suggesting improved thermal stability in the composite matrix [32].

2.6.6 Zeta potential and particle size

Dynamic light scattering and zeta potential measurements were carried out using a Malvern Zetasizer Ultra to determine nanoparticle size distribution and surface charge. High absolute zeta potential values (> ±30 mV) implied colloidal stability and reduced aggregation, essential for biomedical applications [33].

All datasets generated during characterization are publicly available via the Mendeley Data repository (DOI: 10.17632/xtwhbc25hj.2), ensuring transparency and reproducibility.

2.7 *In vitro* evaluation of antidiabetic activity

2.7.1 α-Amylase inhibition assay

The potential α-amylase inhibitory activity of the algal extract, CuO NPs, and nanocomposite scaffolds was assessed using a modified dinitrosalicylic acid (DNSA) method [34]. Each reaction mixture consisted of 200 µL of α-amylase (1 U/mL) and 200 µL of sample at varying concentrations (25–100 µg/mL), pre-incubated at 37°C for 10 minutes. Subsequently, 200 µL of 1% starch (in 0.02 M sodium phosphate buffer, pH 6.9) was added and incubated for 30 minutes. To halt enzymatic activity, 400 µL of DNSA reagent was introduced, followed by heating in a boiling water bath for 5 minutes. Absorbance was measured at 540 nm, and inhibition percentages were calculated accordingly [35].

2.7.2. α-Glucosidase inhibition assay

The α-glucosidase inhibitory activity of the samples was determined using a colorimetric assay involving *p*-nitrophenyl-α-D-glucopyranoside (pNPG) as a substrate [36]. A mixture containing 50 µL of α-glucosidase enzyme (1 U/mL) and 50 µL of each test sample (25–100 µg/mL) was incubated at 37°C for 15 minutes. Test samples included the algal extract, CuO NPs, and starch/PVA/CuO-NPs composites. After pre-incubation, 50 µL of 5 mM pNPG solution (in phosphate buffer, pH 6.8) was added, followed by a 30-minute incubation at 37°C. The reaction was halted by adding 100 µL of 0.1 M Na_2CO_3, producing a yellow color from liberated *p*-nitrophenol. Absorbance was measured at 405 nm. Acarbose served as a positive control. IC_{50} values were determined via non-linear regression [28, 37].

2.8. Statistical processing

All data were statistically analyzed using SPSS v25.0 and GraphPad Prism v9.0. Results were presented as mean ± standard deviation (SD), derived from three independent experimental replicates. One-way analysis of variance (ANOVA) was used to identify significant differences among groups, followed by Tukey's or Dunnett's post hoc tests where appropriate. A p-value less than 0.05 was considered statistically significant. The Pearson correlation test was used to examine the strength of associations between variables. Data distribution normality was assessed using the Shapiro–Wilk test. When data deviated from a normal distribution, they were log-transformed to meet the assumptions of parametric tests. This statistical framework ensured accurate interpretation and reliability of experimental outcomes [38].

3. RESULTS

3.1. UV–Visible Spectroscopy

The UV–Visible spectral analysis (Fig. 1) was conducted using a JASCO V-730 spectrophotometer across 200–800 nm to characterize the *Dictyota* extract and synthesized CuO NPs (NPs). The extract showed a broad absorption profile, peaking at 337 nm (1.482 absorbance), indicative of phytochemicals like polyphenols that likely assisted in nanoparticle formation. The biosynthesized CuO NPs displayed a pronounced peak within 270–300 nm, confirming surface plasmon resonance (SPR), a hallmark of nanoparticle synthesis. Furthermore, CuO NPs showed higher absorbance (2.369 at 800 nm), decreasing steadily toward shorter wavelengths, consistent with the optical behavior of metal oxides. The comparative shift and intensity differences between the extract and CuO NPs validate successful synthesis and highlight phytochemical involvement in nanoparticle reduction and stabilization processes.

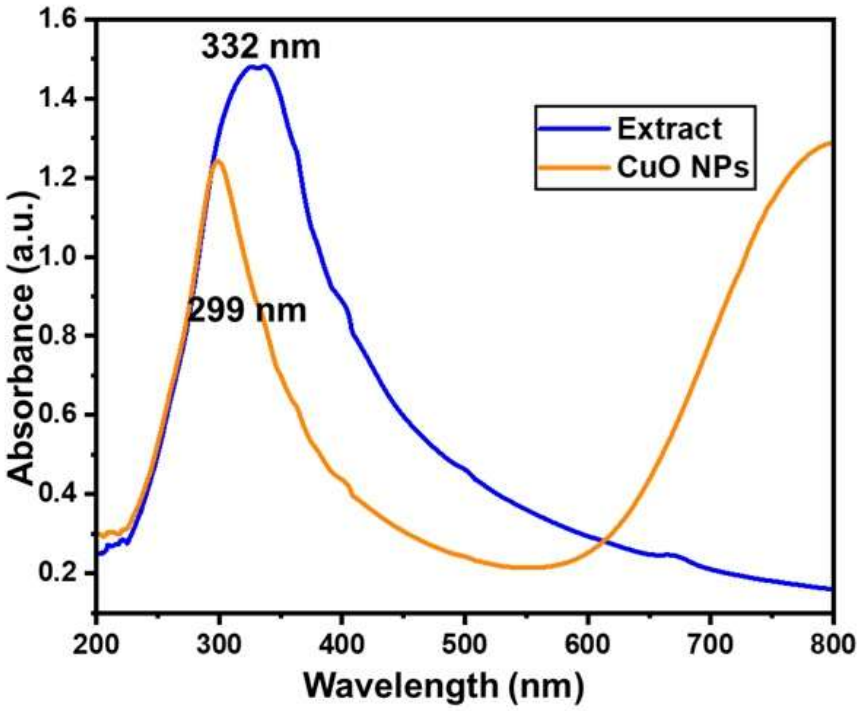

Fig. 1. UV–Visible spectral profiles of algal extract and CuO nanoparticles.

3.2. FTIR analysis

FTIR analysis (Fig. 2) was employed to identify functional groups in both CuO NPs and the CuO-integrated starch/PVA scaffolds. The CuO NPs showed peaks at 2033.36, 1640.64, and 594.02 cm^{-1}, which correspond to Cu–O stretching vibrations, confirming metal oxide formation. Additional signals at 767.66 and 469.77 cm^{-1} further supported the presence of copper–oxygen bonds. In the polymeric scaffold, bands at 3289.72 cm^{-1} (O–H stretching), 1426.07 cm^{-1} (C–H bending), and 110.59 cm^{-1} (C–O–C linkages) reflected the structural characteristics of starch and PVA. Notably, low-frequency signals around 600–400 cm^{-1} indicated successful incorporation of CuO NPs within the polymer matrix. These interactions confirmed that CuO NPs were effectively embedded without disrupting the essential chemical structure of the scaffold.

3.3. XRD analysis

XRD patterns (Fig. 3) confirmed the crystalline nature of biosynthesized CuO NPs and their integration within starch/PVA scaffolds. CuO NPs displayed sharp peaks at 2θ values including 14.03°, 15.60°, 16.25°, and 24.17°, corresponding to the monoclinic CuO phase (JCPDS No. 48-1548). The dominant peak at 24.17° (d-spacing 3.68 Å) confirmed high crystallinity. In contrast, the scaffold exhibited peaks at 21.35° and 29.30°, assigned to starch/PVA structures, with additional minor peaks at 35.78° and 48.52° indicating embedded CuO NPs. Broadening of peaks (FWHM 0.1°–0.6°) in the scaffold suggests reduced crystallinity due to nanoparticle interaction. Overall, the data validate the successful integration of CuO NPs into the scaffold without altering their phase structure, supporting their application in biomedical material design.

3.4. SEM analysis

SEM imaging (Fig. 4) revealed morphological details of CuO NPs and their integration into starch/PVA nanofibers. The synthesized CuO NPs appeared predominantly spherical with slight aggregation, possibly due to surface energy effects. Electrospun nanoscaffolds demonstrated a well-organized fibrous network with uniform fiber distribution at the nanoscale. CuO NPs were distinctly visible as bright spots embedded along the fiber surface, suggesting efficient incorporation into the matrix. The fibers maintained a smooth yet slightly textured morphology, indicating compatibility between the polymer and nanoparticles. Minimal bead formation and consistent diameter were observed, reflecting well-optimized electrospinning parameters. These morphological features affirm the structural integrity and uniform dispersion of CuO NPs, essential for scaffold functionality in biomedical contexts.

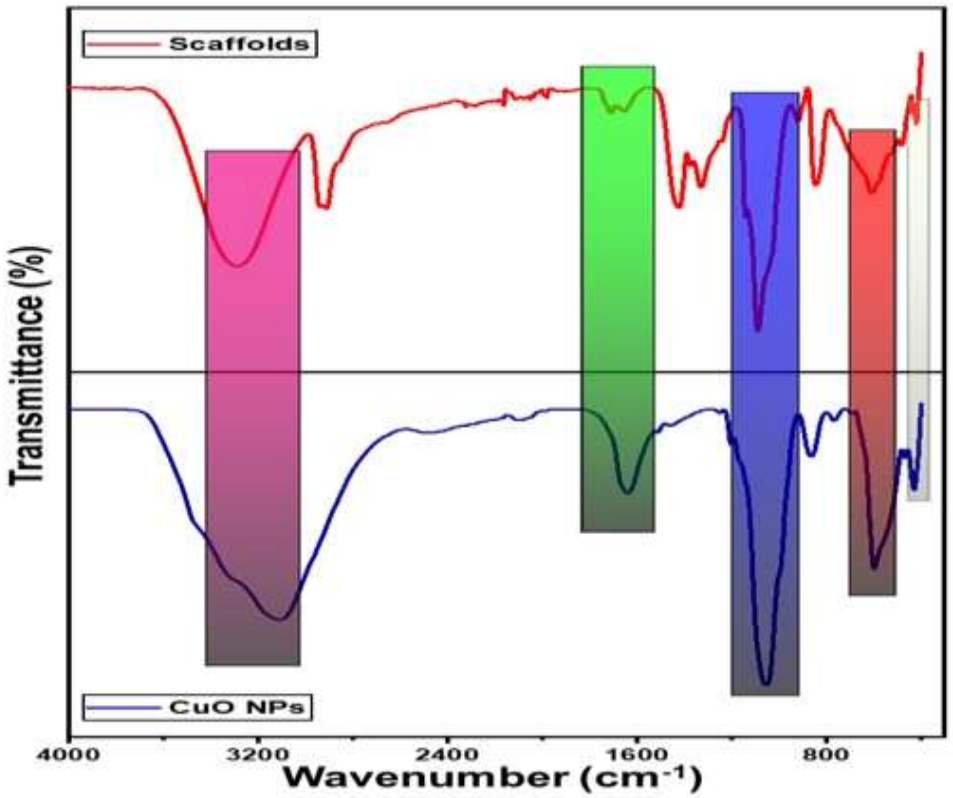

Fig. 2. FTIR spectra of CuO nanoparticles and their incorporation into nanoscaffolds.

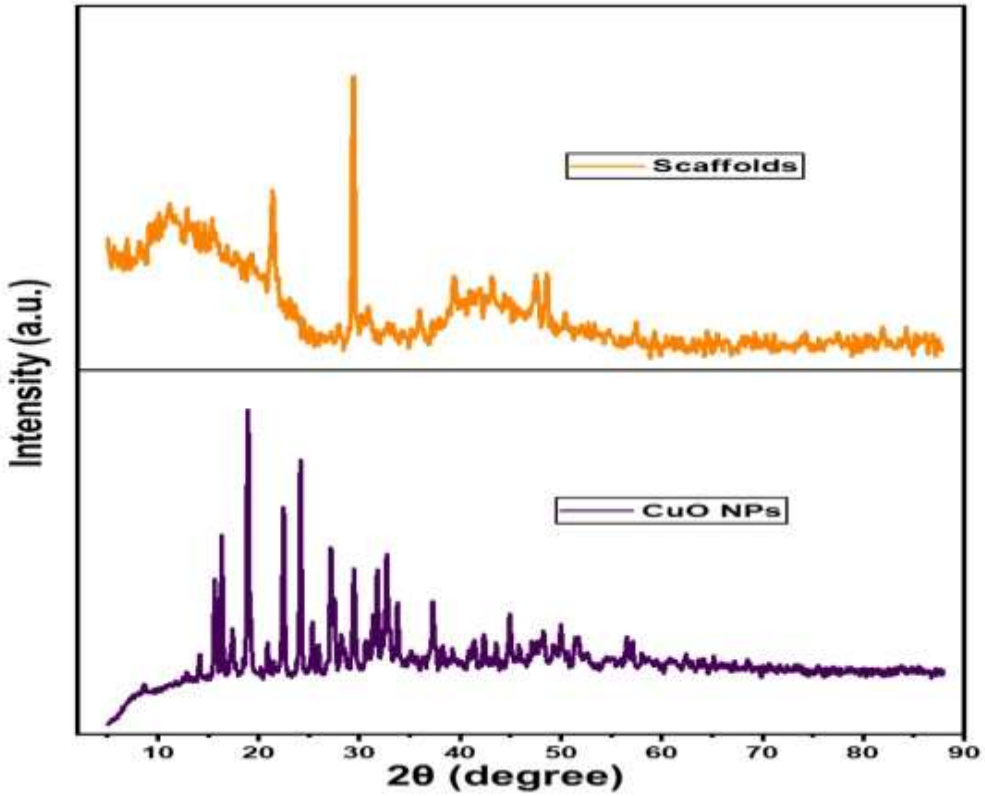

Fig. 3. XRD patterns of synthesized CuO nanoparticles and CuO-loaded scaffolds.

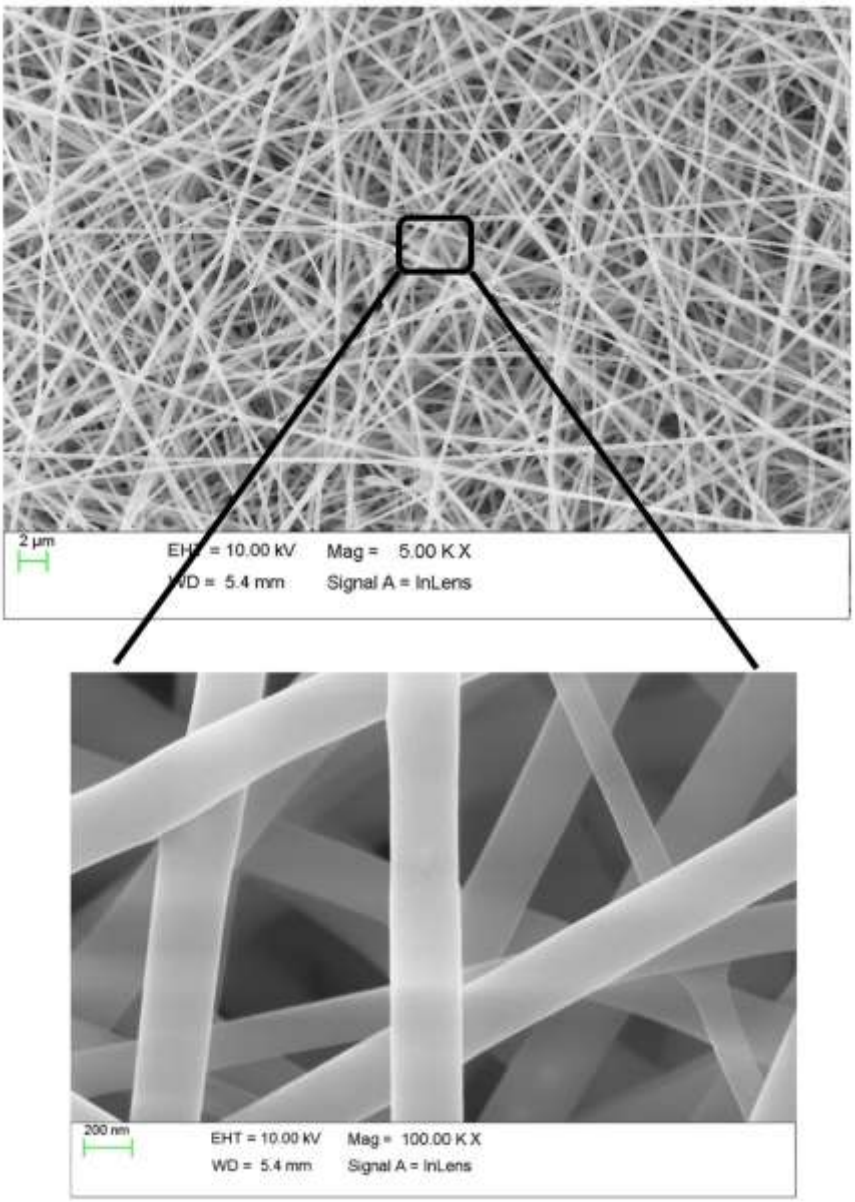

Fig. 4. SEM analysis of fabricated starch/PVA/CuO-NPs nanoscaffolds.

3.5. TGA

Thermal stability (Fig. 5) of the CuO NP-loaded nanoscaffolds was assessed via TGA under nitrogen conditions. The scaffold exhibited an initial weight reduction (7.30%) below 101.7°C, attributed to moisture loss. Major degradation occurred between 234.95°C and 377.09°C, with a prominent decomposition peak at 324.79°C, corresponding to starch/PVA breakdown and accounting for a 37.37% weight loss. Above 400°C, gradual mass decline indicated formation of carbonaceous residue and thermally stable CuO NPs. The residue persisted up to 548.4°C, suggesting the CuO NPs enhanced the scaffold's resistance to thermal decomposition. These findings confirm the thermal reinforcing effect of CuO NPs, making the composite more stable and suitable for high-temperature biomedical and industrial applications.

3.6. Zeta potential and particle size analysis

Dynamic light scattering (DLS) and zeta potential studies assessed the stability and size distribution of CuO NPs in aqueous dispersion. The Z-average particle size was found to be 92.8 nm (Fig. 6) with a polydispersity index (PDI) of 0.688, indicating moderate size variation. Zeta potential measurements revealed a mean surface charge of −20.08 mV with peaks at −37.52 mV and −16.29 mV (Fig. 7). The higher negative value suggested sufficient repulsion to prevent particle aggregation, contributing to colloidal stability. The conductivity value (0.0343 mS/cm) and quality factor (6.538) confirmed accurate measurements. These parameters indicate that the nanoparticles exhibit acceptable dispersion and electrostatic stability, which are crucial for their application in biocompatible systems.

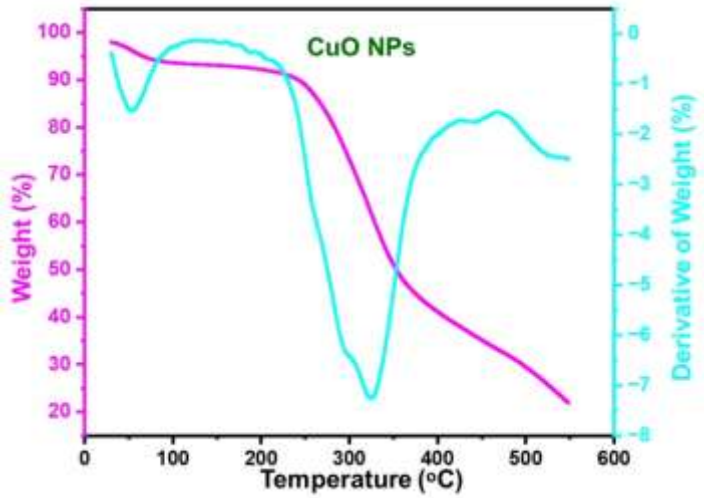

Fig. 5. Thermal degradation behavior of CuO-incorporated nanoscaffolds.

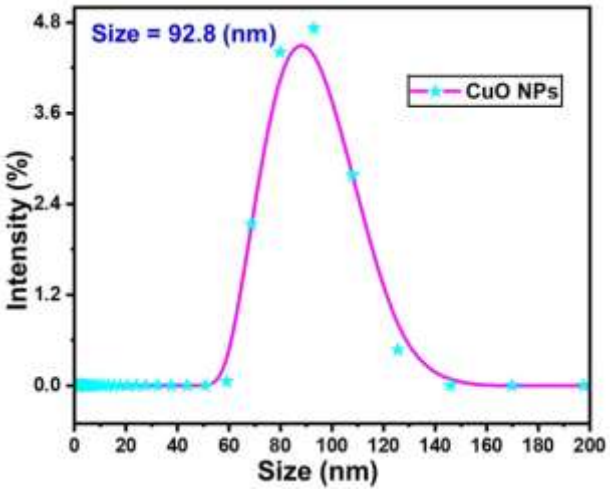

Fig.6. DLS particles size analysis of CuO NPs

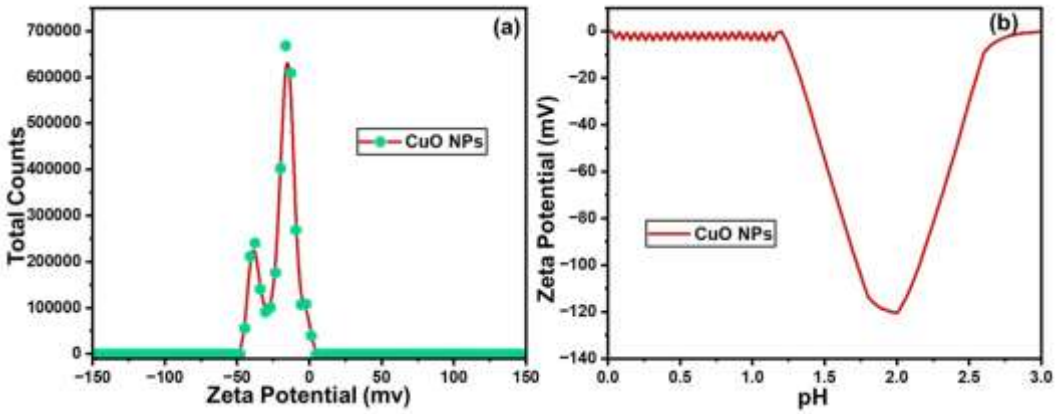

Fig.7. Zeta-potential analysis of CuO NPs

3.7. Antidiabetic activity evaluation

The antidiabetic potential of algal extract, CuO NPs, and starch/PVA/CuO-NPs nanoscaffolds (Fig. 8) was evaluated through their inhibitory effects on α-amylase and α-glucosidase enzymes, key targets for managing

postprandial hyperglycemia. The experiments were conducted at concentrations ranging from 25 to 100 µg/mL, with acarbose as the standard reference.

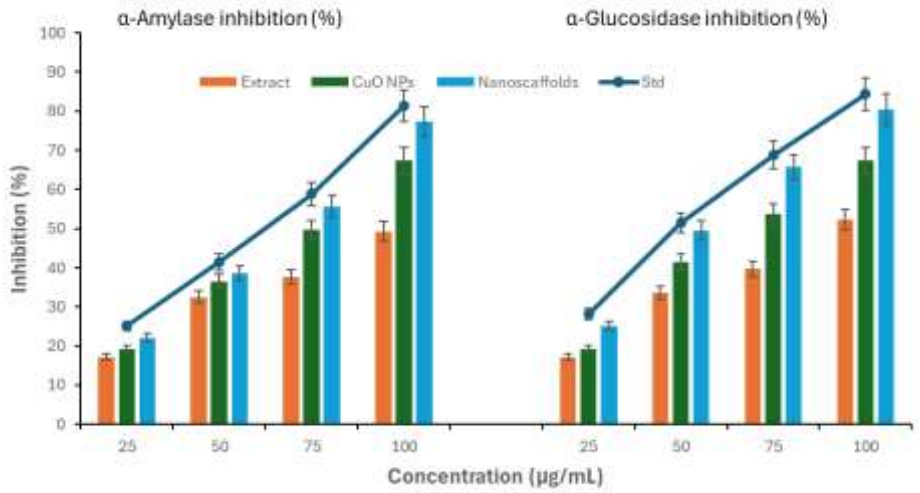

Fig.8. Antidiabetic activity analysis of algal extract, CuNPs and starch/PVA/CuONPs nanoscaffolds

3.7.1. α-Amylase inhibition

The algal extract demonstrated moderate α-amylase inhibition, with activity increasing dose-dependently. At 25 µg/mL, the inhibition was 17.12%, rising to 49.32% at 100 µg/mL. CuO NPs exhibited stronger inhibition, ranging from 19.12% at 25 µg/mL to 67.32% at 100 µg/mL. The starch/PVA/CuO-NPs nanoscaffolds outperformed both the extract and CuO NPs, showing the highest inhibition at all concentrations: 22.12% (25 µg/mL), 38.53% (50 µg/mL), 55.65% (75 µg/mL), and 77.32% (100 µg/mL). These results suggest that the composite nanoscaffolds synergistically enhance the antidiabetic effect, likely due to the combined properties of the polymer matrix and CuO NPs.

3.7.2. α-Glucosidase inhibition

Similar trends were observed in α-glucosidase inhibition. The algal extract showed inhibitory activity of 17.12% at 25 µg/mL, increasing to 52.32% at 100 µg/mL. CuO NPs again displayed higher efficacy, with inhibition rising from 19.12% to 67.32% across the same concentration range. The nanoscaffolds exhibited the most potent inhibition, reaching 80.32% at 100 µg/mL, significantly surpassing the extract and CuO NPs alone. This highlights the nanoscaffolds' potential as a superior antidiabetic agent, possibly due to improved stability and controlled release of active components. The IC_{50} values, derived from non-linear regression, would further clarify the potency of these samples. However, the current data clearly indicate that the starch/PVA/CuO-NPs nanoscaffolds are the most effective, followed by CuO NPs and the algal extract. The enhanced performance of the nanoscaffolds may be attributed to their nanostructured architecture, which maximizes enzyme interaction and inhibition. All tested samples exhibited dose-dependent antidiabetic activity, with the composite nanoscaffolds showing the highest promise for therapeutic applications. Further studies, including *in vivo* assays, are warranted to validate these findings and explore their clinical potential.

4. DISCUSSION

The present study successfully demonstrated the green synthesis of CuO NPs using *Dictyota* extract, followed by their incorporation into starch/PVA-based nanoscaffolds. A comprehensive physicochemical characterization and bioactivity evaluation underscored the potential of these materials for biomedical applications, particularly for antidiabetic therapy.

UV–Visible spectroscopy served as an initial confirmation of nanoparticle formation. The *Dictyota* extract exhibited a broad absorption band centered at 337 nm, a signature consistent with phytochemicals such as polyphenols and flavonoids known for their reducing and capping abilities. The biosynthesized CuO NPs showed a distinct absorption peak within 270–300 nm, attributable to surface plasmon resonance (SPR) phenomena inherent to metal oxide nanoparticles. This spectral shift, alongside the higher absorbance observed at longer wavelengths (~800 nm), suggests successful reduction and stabilization of CuO by bioactive compounds in the algal extract. Such optical properties confirm that the extract not only mediated nanoparticle synthesis but also influenced their electronic structure and optical behavior, crucial for functional performance in applications like sensing and catalysis [39-45].

FTIR analysis provided further evidence for the chemical interactions occurring during synthesis and composite fabrication. The characteristic Cu–O stretching vibrations detected between 594 and 2033 cm^{-1} confirmed the formation of copper oxide in its monoclinic phase. Simultaneously, the polymer scaffold spectra revealed functional groups typical of starch and PVA, such as hydroxyl (O–H) and ether (C–O–C) linkages. Importantly, the appearance of low-frequency bands (400–600 cm^{-1}) in the composite scaffold indicated successful embedding of CuO NPs without disturbing the polymeric backbone. This suggests strong interfacial compatibility, likely due to hydrogen bonding or electrostatic interactions, which is vital to maintain scaffold integrity while imparting nanoparticle-driven functionalities [46-49].

XRD patterns substantiated the crystalline nature of the synthesized CuO NPs and their incorporation into the starch/PVA matrix. Sharp diffraction peaks at specific 2θ angles confirmed the monoclinic CuO phase, consistent with reference standards. The presence of distinct CuO peaks in the composite scaffold, along with typical starch/PVA peaks, confirmed that the nanoparticles retained their crystal structure upon integration. However, the observed broadening of peaks in the scaffold suggested a slight reduction in crystallinity, possibly caused by nanoparticle-polymer interactions disrupting the orderly packing of polymer chains. This phenomenon often benefits biomedical scaffolds by enhancing flexibility and facilitating controlled release of active agents [50-55].

SEM micrographs revealed that CuO NPs were mostly spherical, albeit slightly aggregated, which could be attributed to their surface energy and the absence of strong stabilizing agents beyond phytochemicals. The electrospun starch/PVA nanofibers displayed a well-defined, uniform fibrous network with minimal bead formation and consistent fiber diameter, indicating optimized electrospinning parameters. CuO NPs appeared as bright, dispersed clusters on fiber surfaces, reflecting efficient embedding. This uniform dispersion is critical for ensuring consistent biological responses and mechanical properties. Moreover, the smooth yet textured fiber morphology suggests good compatibility between the polymer matrix and nanoparticles, a prerequisite for mechanical robustness and biocompatibility in tissue engineering or drug delivery applications [56-61].

Thermogravimetric analysis demonstrated that the CuO NP-loaded scaffolds exhibited enhanced thermal stability compared to neat polymers. Initial weight loss below 102°C corresponded to moisture evaporation, typical for hydrophilic biopolymers like starch and PVA. Major decomposition occurred between ~235°C and 377°C, reflecting polymer backbone breakdown. Notably, the presence of CuO NPs resulted in a thermally stable residue persisting up to ~548°C, signifying their role as heat-resistant fillers. This thermal reinforcement implies that CuO NPs not only provide functional properties but also improve scaffold durability under physiological and processing conditions, broadening their applicability [62-66].

Dynamic light scattering data indicated that the CuO NPs possessed an average hydrodynamic size of approximately 93 nm, within the expected nanometric range favorable for biomedical interactions. A polydispersity index near 0.7 reflected moderate size distribution, which is acceptable for most applications. The zeta potential values ranged widely but centered around −20 mV, indicative of moderate surface charge sufficient to confer electrostatic repulsion and colloidal stability. Such stability is critical to prevent aggregation in physiological media, thus ensuring consistent biological activity and effective delivery when incorporated into scaffolds [67-69].

The most compelling biological results emerged from evaluating the inhibition of α-amylase and α-glucosidase enzymes, key regulators of carbohydrate metabolism and targets for antidiabetic therapy. The *Dictyota* extract exhibited moderate inhibitory effects that increased with concentration, consistent with previous reports on marine algal bioactives. Notably, CuO NPs displayed enhanced inhibition, likely due to their high surface area and potential to interact with enzyme active sites or alter substrate binding. Strikingly, the starch/PVA/CuO-NPs nanoscaffolds showed superior inhibition across all tested concentrations, surpassing both the extract and nanoparticles alone [70-73].

This enhanced bioactivity may arise from several factors: first, the scaffold's nanofibrous architecture provides a large surface area for enzyme interaction; second, the controlled release and stabilization of active CuO NPs within the polymer matrix may prolong their enzymatic effects; and third, potential synergistic effects between polymer components and nanoparticles may amplify inhibition. The dose-dependent responses underscore the therapeutic promise of these composite scaffolds for managing postprandial hyperglycemia, a critical factor in diabetes control.

Collectively, the results affirm that *Dictyota* extract-mediated CuO NPs can be effectively synthesized, characterized, and embedded into starch/PVA scaffolds, yielding composites with favorable physicochemical properties and significant antidiabetic activity. The scaffold's structural integrity, thermal stability, and enzyme inhibitory potential position it as a promising candidate for biomedical applications aimed at diabetes management. Further investigations, including detailed kinetic studies, IC_{50} determinations, cytotoxicity assays, and *in vivo* evaluations, will be essential to fully elucidate the therapeutic potential and safety profile of these nanocomposites. Additionally, exploring other biological activities and optimizing scaffold formulations could expand their applicability in regenerative medicine and drug delivery.

5. CONCLUSION

This study successfully demonstrated the green synthesis of CuO NPs using *Dictyota* algal extract and their incorporation into starch/PVA nanofiber scaffolds via electrospinning. The synthesized CuO NPs exhibited characteristic surface plasmon resonance and crystallinity, as confirmed by UV-Vis and XRD analysis, while FTIR revealed the presence of bioactive phytochemicals responsible for nanoparticle stabilization. The nanoscaffolds displayed uniform fiber morphology and enhanced thermal stability, making them suitable for biomedical applications. *In vitro* antidiabetic assays revealed that the starch/PVA/CuO-NPs nanoscaffolds exhibited superior α-amylase and α-glucosidase inhibition compared to the algal extract and bare CuO NPs, suggesting a synergistic effect between the polymeric matrix and nanoparticles. The dose-dependent enzyme inhibition and low IC_{50} values highlight their potential as an effective alternative to conventional antidiabetic drugs. These findings underscore the promise of marine algae-mediated nanotechnology in developing biocompatible, eco-friendly therapeutics for diabetes management. Future research should focus on *in vivo* studies to validate efficacy, biosafety, and long-term stability for clinical translation.

Ethical Declaration: Not Applicable

Data Availability Statement: The full dataset of physiochemical characterization associated with this work is published in Mendeley Data (doi: 10.17632/xtwhbc25hj.2). **Disclosure:** The material characterization data and figures (e.g., UV, SEM, FTIR, XRD, TGA, Zeta Potential and particle sizer) presented here were generated from a common dataset and are being reused across multiple related studies on nanomaterials. All biological and environmental analyses and conclusions are original to each manuscript.

Conflicts of Interest: The authors declare no conflicts of interest.

REFERENCES

[1] Huang Y, Guo H, Liu Y, Jin W, Palanisamy CP, Pei J, Oz F, El-Aty AMA. Effects of Natural Polysaccharides on the Gut Microbiota Related to Human Metabolic Health. Molecular Nutrition & Food Research. 2025; e202400792.

[2] Prabhakaran P, Palanisamy CP, Shanmugam A, Damodharan P, Swaminathan H, Devaraj D, Ahalliya RM, Kanniappan GV. Isolation, structural characterization, and molecular docking studies on the bioactive compound from n-Hexane extract of Emilia sonchifolia (L.) DC against the pancreatic cancer target Aurora 2 Kinase. Journal of Complementary and Integrative Medicine. 2024; 22(1): 0290.

[3] Jiang H, Kumarasamy RV, Pei J, Raju K, Kanniappan GV, Palanisamy CP. Integrating engineered nanomaterials with extracellular vesicles: Advancing targeted drug delivery and biomedical applications. Frontiers in Nanotechnology. 2024; 6: 1513683.

[4] Guo H, Liu Y, Wan T, Song D, Palanisamy CP, Geng J, Pei J, Özmen S, El-Aty AMA. Toward personalized cancer management: Role of precision nutrition–diet interventions. Journal of Functional Foods. 2024; 123: 106584.

[5] Natarajan SR, Krishnamoorthy R, Alshuniaber MA, Al-Anazi KM, Farah MA, Rajagopal P, Palanisamy CP, Veeraraghavan VP, Jayaraman S. Identification of FOXM1 as a novel protein biomarker and therapeutic target for colorectal cancer progression: Evidence from immune infiltration and bioinformatic analyses. International Journal of Biological Macromolecules. 282 (Part 4): 137201.

[6] Rajendran MS, Jayaraman S, Khan JM, Jasmine S, Prabhakaran RK, Raju MV, Chandrasekaran MK, Ahalliya RM, Kannappan P, Palanisamy CP, Kanniappan GV. Investigating the colon toxicity and carcinogenic role of monosodium glutamate compared with Dimethylhydrazine in male Wistar rats: Exploring the link to childhood colon cancer risk. Journal of King Saud University - Science. 2024; 36(11): 103507.

[7] Kumarasamy RV, Natarajan P, Umapathy VR, Roy JR, Rab SO, Saeed M, Panagal M, Mironescu M, Srinivasan GP, Palanisamy CP. Clinical Applications and Therapeutic Potentials of Advanced Nanoparticles: A Comprehensive Review on Completed Human Clinical Trials. Frontiers in Nanotechnology. 2024; 6:1479993.

[8] Jin W, Pei JJ, Roy JR, Jayaraman S, Ahalliya RM, Kanniappan GV, Mironescu M, Palanisamy CP. Comprehensive review on single-cell RNA sequencing: A new frontier in Alzheimer's disease research. Ageing Research Reviews. 2024; 274: 102454.

[9] Pei J, Palanisamy CP, Jayaraman S, Natarajan PM, Umapathy VR, Roy JR, Panagal M, Jayaraman S. Curcumin-loaded polymeric nanomaterials as a novel therapeutic strategy for Alzheimer's disease: A comprehensive review. Ageing Research Reviews. 2024; 99: 102393.

[10] Pei J, Palanisamy CP, Jayaraman S, Natarajan PM, Umapathy VR, Roy JR, Thalamati D, Ahalliya RM, Kanniappan GV, Mironescu M. A comprehensive review on starch-based Sustainable Edible Films Loaded

with Bioactive Components for Food Packaging. International Journal of Biological macromolecules. 2024; 274 (Part-1): 133332.
[11] Palanisamy CP, poompradub S, Sansanaphongpricha K, Subramani K, Sonsudin F. Increased expression levels of PDGF and VEGF magnify the wound healing potential facilitated by biogenic synthesis of silver nanoparticles. Nano-Structures & Nano-Objects. 2024; 39: 101236.
[12] Pei J, Palanisamy CP, Jayaraman S, Natarajan PM, Umapathy VR, Roy JR, Thalamati D, Ahalliya RM, Kanniappan GV, Mironescu M. Proteomics Profiling of Extracellular Vesicle for Identification of Potential Biomarkers in Alzheimer's Disease: A Comprehensive Review. Ageing Research Reviews. 2024; 99: 102359.
[13] Xi J, Wang T, Xian P, Liu X, Du M, Yang H, Palanisamy CP, Lin W, Long Q. Proteomic insights uncover enhanced neurotherapeutic potential in conditioned mesenchymal stem cell-derived extracellular vesicles. Extracellular Vesicle. 2024; 3: 100037.
[14] Pei J, Natarajan PM, Umapathy VR, Swamikannu B, Sivaraman NM, Krishnasamy L, Palanisamy CP. Advancements in the synthesis and functionalization of zinc oxide-based nanomaterials for enhanced oral cancer therapy. Molecules. 2024; 29(11): 2706.
[15] Gatasheh MK, Natarajan SR, Krishnamoorthy R, Alsulami TS, Rajagopal P, Palanisamy CP, Veeraraghavan VP, Jayaraman S. Molecular analysis to identify novel potential biomarkers as drug targets in colorectal cancer therapy: an integrated bioinformatics analysis. Molecular and Cellular Oncology. 2024; 11(1): 2326699.
[16] Pei J, Yan Y, Jayaraman S, Rajagopal P, Natarajan PM, Umapathy VR, Gopathy S, Roy JR, Sadagopan CS, Thalamati D, Palanisamy CP, Mironescu M. A review on advancements in the application of starch-based nanomaterials in biomedicine: Precision drug delivery and cancer therapy. International Journal of Biological Macromolecules. 2024; 130746.
[17] Natarajan PM. Dental Bioinformnatics-Current Scope and Future perspectives. Research Journal of Pharmacy and Technology. 2022;15(5):2351-6.
[18] Natarajan PM, Umapathy VR, Murali A, Swamikannu B. (2022). Computational Simulations of Identified marine-derived Natural Bioactive Compounds As Potential Inhibitors of Oral Cancer. Future Science OA. 2022; 8(3).
[19] Natarajan PM, Umapathy VR. Role of transcriptomics in the study of oral cancer. Frontiers in Oral Health. 2025; 6:1524364.
[20] Natarajan PM, Swamikannu B, Sivaraman NM, Stylin AGSQ. Prevention of Oral Cancer: A Comprehensive Guide. Journal of Pharmacy and Bioallied Sciences. 2024; 16(5): S4239-S4241.
[21] Pei JJ, Yan Y, Palanisamy CP, Jayaraman S, Natarajan PM, Umapathy VR, Gopathy S, Roy JR, Sadagopan JC, Thalamati D, Mironescu M. Materials-based drug delivery approaches: Recent advances and future perspectives. Green Processing and Synthesis. 2024; 13: 20230094.
[22] Pei JJ, Deng W, Liu Y, Guo Y, Chen J, Abdu H, Khan MR, Palanisamy CP, El-Aty AM. A Comprehensive Review of Cornus officinalis: Health Benefits, Phytochemistry, and Pharmacological Effects for Functional Drug and Food Development. Frontiers in Nutrition. 2023; 10: 1309963.
[23] Alugoju P, Palanisamy CP, Anthikapalli NVA, Jayaraman S, Prasanskulab A, Chuchawankul S, Dyavaiah M, Tencomnao T. Exploring the anti-aging potential of natural products and plant extracts in budding yeast Saccharomyces cerevisiae: A review. F1000Research. 2023; 12: 1265.
[24] Lavanya M, Krishnamoorthy R, Alshuniaber MA, Manoharadas S, Palanisamy CP, Veeraraghavan VP, Jayaraman S, Rajagopal P, Padmini R. Formulation, characterization and evaluation of gelatin-syringic acid/zinc oxide nanocomposite for its effective anticancer, antioxidant and anti-inflammatory activities. Journal of King Saud University-Science. 2023; 35: 102909.
[25] Palanisamy CP, Poompradub S, Sansanaphongpricha K, Jayaraman S, Subramani K, Sonsudin F. Biosynthesis of silver nanoparticles (AgNPs) using ethanolic extract of Nigella sativa (L.) seeds promotes wound healing via PDGF and VEGF signalling pathways activation. Biocatalysis and Agricultural Biotechnology. 2023; 54: 102970.
[26] Natarajan PM. Computational Studies on Recent Congeners of Fluoroquinolones and Nitroimidazoles for Their Use in Periodontal Therapy. Journal of Pharmacy and Bioallied Sciences. 2024; 16(5): S4731-S4740.
[27] Natarajan PM, Bhuminathan S, Rajan R, Bindu K, Loganathan K, Veerakumar R. The Crucial Role of Smoking Cessation in Preventing Oral Cancer. Journal of Pharmacy and Bioallied Sciences. 2024; 16(5): S4245-S4247.
[28] Natarajan PM, Bhuminathan S, Leela B, Bindu K, Loganathan K, Ramachandran V. Smoking and its Role in Oral Cancer. Journal of Pharmacy and Bioallied Sciences 16(5): S4242-S4244.
[29] Vidhyarekha U, Natarajan PM, Bhuminathan S, Sabarinathan J, Suba R, Vijayalakshmi P. Role of artificial intelligence in Oral Cancer. Advances in Public Health. 2024. 2024: 3664408.
[30] Ganesan A, Kumar NG, Natarajan PM, Gauthaman J. Automated classification of elongated styloid processes using deep learning models-an artificial intelligence diagnostics. Frontiers in Oral Health. 2025; 5: 1424840.
[31] Umapathy VR, Natarajan PM, Swamikannu B. Regenerative Strategies in Dentistry: Harnessing Stem Cells, Biomaterials and Bioactive Materials for Tissue Repair. Biomolecules. 2025; 15: 546.

[32] Ganesan A, Kumar NG, Natarajan PM. Solanum trilobatum leaf extract-derived silver nanoparticles downregulate the PI3K/AKT/mTOR signaling pathway and attenuate oral squamous cell carcinoma cell proliferation. Journal of Herbmed Pharmacology. 2024; 13(2): 300-307.
[33] Perumal MKK, Renuka RR, Subbiah SK, Natarajan PM. Artificial intelligence-driven clinical decision support systems for early detection and precision therapy in oral cancer: a mini review. Frontiers in Oral Health. 2025; 6: 1592428.
[34] Ramesh E, Ganesan A, Lakshmi KC, Natarajan PM. Artificial intelligence-based diagnosis of oral leukoplakia using deep convolutional neural networks Xception and MobileNet-v2. Frontiers in Oral Health. 2025; 6: 1414524.
[35] Ganesan A, Kumar NG, Natarajan PM. Anticancer activity of silver nanoparticles synthesized from aqueous leaf extract of Solanum trilobatum (Purple fruit pea eggplant) on human oral cancer cells. Journal of Herbmed Pharmacololgy. 2024; 13(2): 260-268.
[36] Daniel Raja FS, Abraham L, Rangasamy K, Saikia K, Rathankumar AK, Mironescu M, Mironescu I, Palanisamy CP, Kanniappan GV. Next-Generation Microbiome Therapeutics: Psychobiotics and Fecal Microbiota Transplants (FMT) for Mental Health Treatment. Frontiers in Cellular and Infection Microbiology. 2026; 16: 1719357.
[37] Dharmaprakash S, Gunasekaran VP, Sivaramakrishnan R, Kanniappan GV, Jayaraman S, Mironescu M, Rajabathar JR, Mironescu ID, Palanisamy CP. Marine macroalgae-mediated ultrasonic-assisted green synthesis of CuO nanoparticles embedded in starch/PVA electrospun nanoscaffolds for in vitro α-amylase and α-glucosidase inhibitory activity. Scientific Reports. 2026.
[38] Surendran N, Chandrasekaran G, Raju MV, Chandrasekaran MK, Ahalliya RM, Palanisamy CP, Kanniappan GV, Arcot R, Alharbi NS, Thiruvengadam M. Anti-inflammatory potential of ethanolic extract of Maranta arundinacea L.: Insights from COX-2 modulation and oxidative stress analysis. South African Journal of Botany. 2026; 195: 142-151.
[39] Pei J, Senthilkumar MV, Hessini K, Subramaniyam S, Sivaramakrishnan R, Kanniappan GV, Jayaraman S, Palanisamy CP. Green fabrication of starch/PVA/CuO nanoscaffolds using marine macroalgae extract for enhanced anti-inflammatory activity. Sustainable Chemistry and Pharmacy. 2026; 51: 102397.
[40] Balasubramanian V, Loganathan L, Muthuswamy K, Viswanathan TM, Raju MV, Chandrasekaran MK, Ahalliya RM, Poorasamy J, Palanisamy CP, Dominic S, Kanniappan GV. Anticancer therapeutic efficacy of PEGylated β-galactosidase from Aspergillus terreus in DMBA-induced breast cancer: Toxicological, molecular and histopathological evaluation in Wistar rats. International Journal of Biological Macromolecules. 2026; 360: 151856.
[41] Jayaraman S, Eswaran A, Rajagopal P, Palanisamy CP, Veerakumar P, Veeraraghavan VP, Sirasanagandla SR. Neuroendocrine-associated epigenetic factors in cellular senescence: mechanisms and therapeutic implications. Biogerontology. 2026; 27(2): 64.
[42] Ponnusamy B, Rajagopal P, Palanisamy CP, Veeraraghavan VP, Jayaraman S. Mechanistic Exploration of the anticancer activity of Justicia adhatoda Plant Leaf Ethanolic Extract against Colon Cancer Cells: An in silico and in vitro Approach. Asian Pacific Journal of Cancer Prevention. 2026; 27(3): 1069-1080.
[43] Pei J, Saran VS, Sivaramakrishnan R, Kanniappan GV, Pandurangan V, Jayaraman S, Dhayalan VK, Mironescu M, Mironescu ID, Palanisamy CP. Ultrasonic-assisted, Sargassum ilicifolium (brown marine macroalgae)-mediated biogenic synthesis of CuO nanoparticles incorporated in starch/PVA electrospun nanoscaffolds: In vitro safety and antioxidant efficacy assessment. Bioorganic Chemistry. 2026; 173: 109679.
[44] Raj MAPA, Subramaniyam S, Kanniappan GV, Jayaraman S, Palanisamy CP. Sustainable fabrication of starch/PVA/CuO electrospun nanoscaffolds from Turbinaria ornata (marine macroalgae) extract: Physicochemical characterization and antidiabetic evaluation. Kuwait Journal of Science. 2026; 53(2): 100545.
[45] Pei J, Ganesh NS, Subramaniyam S, Sivaramakrishnan R, Kanniappan GV, Jayaraman S, Palanisamy CP. Sustainable fabrication of starch/PVA/CuO electrospun nanoscaffolds from Padina tetrastromatica (Brown macroalgae) extract: Physicochemical characterization and antidiabetic assessment. Sustainable Chemistry One World. 2026; 9: 100195.
[46] Sakthiraj A, Sivaramakrishnan R, Subramaniyam S, Kanniappan GV, Pandurangan V, Jayaraman S, Dhayalan VK, Mironescu M, Mironescu ID, Palanisamy CP. Starch/PVA electrospun nanoscaffolds loaded with ultrasonic-assisted green-synthesis of CuO nanoparticles from marine macroalgae (Gracilaria corticata) extract: Cytotoxicity and antioxidant analysis. Chemical Physics Impact. 2026; 12: 101018.
[47] Raju M, Chandrasekaran MK, Loganathan L, Ahalliya RM, Mironescu M, Mironescu ID, Palanisamy CP, Kanniappan GV. Lipid remodeling and ferroptosis in phosphatidylcholine-mediated tumor–stroma crosstalk. Frontiers in Molecular Biosciences. 2026; 13: 1742305.
[48] Kunamalla R, Panagal M, Palanisamy CP. Biogenic synthesis and fabrication of starch/PVA/CuO electrospun nanoscaffolds from Sargassum ilicifolium (brown marine macroalgae) extract for anticancer activity on HT-29 and MCF-7 cancer cells. Biocatalysis and Agricultural Biotechnology. 2026; 72: 103923.
[49] Pei J, Govindaraj H, Sivaramakrishnan R, Kanniappan GV, Pandurangan V, Dhayalan VK, Mironescu M, Mironescu ID, Jayaraman S, Palanisamy PC. Sustainable fabrication of biopolymer-based (starch/PVA)

nanoscaffolds loaded with green-synthesized CuO nanoparticles from Sargassum wightii (marine macroalgae): Cytocompatibility and antioxidant activity. Biomaterials Advances. 2026; 182: 214660.
[50] Pei J, Perumal NC, Meng P, Long Q, Palanisamy CP. Extracellular vesicle-based biosensors for Alzheimer's disease: A new frontier in precision diagnostics. Ageing Research Reviews. 2026; 113: 102904.
[51] Shree P, Sivaramakrishnan R, Kanniappan GV, Pandurangan V, Jayaraman S, Dhayalan VK, Mironescu M, Mironescu ID, Palanisamy CP. Antioxidant and biocompatible CuO-starch/PVA nanoscaffolds via ultrasonic green synthesis using Turbinaria conoides (brown marine macroalgae). Medicine in Drug Discovery. 2025; 28: 100238.
[52] Gong J, Lin J, Guan T, Pei J, Palanisamy CP, El-AtyFrom AMA. selenium tolerance to nanoplastic antagonism: Comprehensive characterization of L. casei SNUT1 and its extracellular vesicle–nanoselenium complex. Food Bioscience. 2025; 74: 107749.
[53] Poochi SP, Sundarraj R, Raju MV, Chandrasekaran MK, Ahalliya RM, Palanisamy CP, Kanniappan GV, Kondapavuluri BK, Thiruvengadam M. Harnessing Nature: Computational and Experimental Insights Into *Ipomoea obscura* Metabolites for Bladder Cancer Therapy. Chemistry and Biodiversity. 2025; 0: e00909.
[54] Dugganaboyana GK, Kannankumar MKG, Shivaramakrishna S, Raju MV, Chandrasekaran MK, Ahalliya RM, Panneerselvam N, Palanisamy CP, Kanniappan GV. Phytochemical insights, antioxidant activity and therapeutic potential of Cassia senna against prostate cancer in Wistar albino rats. Discover Applied Sciences. 2025; 7:1206.
[55] Natarajan SR, Krishnamoorthy R, Alshuniaber MA, Gatasheh MK, Rajagopal P, Veeraraghavan VP, Palanisamy CP, Jayaraman S. KDM1A Facilitates Oncogenic Potential in Colorectal Cancer Progression Through the Activation of AXIN/GSK3β/β-Catenin Signaling Pathways: Evidence From Integrated Transcriptomics and In Vitro Studies. The Journal of Gene Medicine. 2025; 27(11): e70053.
[56] Guan T, Gong J, Lin J, Palanisamy CP, Jinjin Pei J, El-Aty AMA. Machine learning-driven multimodal optimization of selenium biotransformation and flavor profiling in fermented apple–Yacon functional beverages. Innovative Food Science & Emerging Technologies. 2025; 105: 104198.
[57] Natarajan SR, Krishnamoorthy R, Alshuniaber MA, Alsulami TS, Gatasheh MK, Rajagopal P, Palanisamy CP, Govindan R, Veeraraghavan VP, Jayaraman S. ABCE1 facilitates tumour progression via aerobic glycolysis and inhibits cell death in human colorectal cancer cells through the p53 signalling pathway. Scientific Reports. 2025; 15: 24674.
[58] Huang Y, Guo H, Liu Y, Jin W, Palanisamy CP, Pei J, Oz F, El-Aty AMA. Effects of Natural Polysaccharides on the Gut Microbiota Related to Human Metabolic Health. Molecular Nutrition & Food Research. 2025; 69:e202400792.
[59] Poornima K, Meenakshi K.C, Manikandan V.R, Shankari G, Prabhu D, Rathi M.A, Palanisamy CP, Balaji R, Gopalakrishnan V.K. Exploring the anticancer potential of Jerantinine A from *Tabernaemontana coronaria* against prostate, breast, and ovarian cancers: A computational approach. *Journal of Complementary and Integrative Medicine*, 2025 22(2): 363–372.
[60] Palanisamy CP, Poompradub S, Sansanaphongpricha K, Jayaraman S, Subramani K. Faridah Sonsudin gGreen synthesis of Nigella sativa-mediated silver nanoparticles for enhanced antibacterial activity and wound healing: Mechanistic insights and biomedical applications. Environmental Nanotechnology, Monitoring & Management. 2025; 24: 101085.
[61] Surendran N, Raju MV, Chandrasekaran MK, Ahalliya RM, Palanisamy CP, Chandrasekaran G, Kanniappan GV. Physicochemical characterization of starch from Maranta arundinacea L.(arrowroot) rhizomes and its inhibition of COX-2: In vivo validation. Bioactive Carbohydrates and Dietary Fibre. 2025; 33: 100465.
[62] Kannappan P, Chandrasekaran MK, Raju MV, Gopalakrishnan S, Dhamodharan P, Ahalliya RM, Palanisamy CP, Raju B, Kanniappan GV. Exploring the anticancer potential of Jerantinine A from Tabernaemontana coronaria against prostate, breast, and ovarian cancers: a computational approach. Journal of Complementary and Integrative Medicine. 2025; 22(02): 363-372.
[63] Pei J, Kumarasamy RV, Jayaraman S, Kanniappan GV, Long Q, Palanisamy CP. Quercetin-functionalized nanomaterials: Innovative therapeutic avenues for Alzheimer's disease management. Ageing Research Reviews. 2025; 104: 102665.
[64] Jayaraman S, Prasad M, Natarajan SR, Krishnamoorthy R, Alshuniaber MA, Gatasheh MK, Veeraraghavan VP, Rajagopal P, Palanisamy CP. Molecular mechanisms underlying the effects of beta-sitosterol on TGF-β1/Nrf2/SIRT1/p53-mediated signaling in the kidney of a high-fat diet and sucrose-induced type-2 diabetic rat. Chemico-Biological Interactions. 2025; 411: 111443.
[65] Umapathy V, Dhanavel A, Kesavan R, Natarajan PM, Bhuminathan S, Vijayalakshmi P. Anticancer Potential of the Principal Constituent of Piper nigrum, Piperine: A Comprehensive Review. Cureus. 2024; 16(2): e54425.
[66] Umapathy VR, Swamikannu B, Natarajan PM, Devi R, Nandini MS, Vimalarani, Vijayalakshmi P. In Silico Molecular Docking of Ocimum sanctum Phytochemicals: Targeting Key Biomarkers in Oral Cancer. Journal of Pharmacy and Bioallied Sciences. 2024; 16(5): S4792-S4799.

[67] Swamikannu B, Umapathy VR, Natarajan PM, Nandini MS, Stylin AGSQ, Vimalarani V, Rajinikanth S. Unlocking the Therapeutic Benefits of Artemisia Annua: A Comprehensive Overview of its Medicinal Properties. Journal of Pharmacy and Bioallied Sciences. 2024; 16(5): S4248-S4253.
[68] Yadalam PK, Arumuganainar D, Natarajan PM, Ardila CM. Artificial intelligence-powered prediction of AIM-2 inflammasome sequences using transformers and graph attention networks in periodontal inflammation. Scientific Reports. 2025; 15: 8733.
[69] Yadalam PK, Chatterjee S, Natarajan PM, Ardila CM. Comparison of light gradient boosting and logistic r egression for interactomic hub genes in Porphyromonas gingivalis and Fusobacterium nucleatum-induced periodontitis with Alzheimer's disease. Frontiers in Oral Health. 2025; 6:1463458.
[70] Yadalam PK, Natarajan PM, Ardila CM. Variational graph autoencoder for reconstructed transcriptomic data associated with NLRP3 mediated pyroptosis in periodontitis. Scientific Reports. 2025; 15: 1962.
[71] Prasad M, Jayaraman S, Natarajan SR, Veeraraghavan VP, Krishnamoorthy R, Gatasheh MK, Palanisamy CP, Elrobh M. Piperine modulates IR/Akt/GLUT4 pathways to mitigate insulin resistance: Evidence from animal and computational studies. International Journal of Biological Macromolecules. 2023; 253: 127242.
[72] Palanisamy CP, Pei JJ, Phaniendra A, Venkata AAN, Jayaraman S, Veeraragahavan VP, Sridevi G, Roy JR, Janaki CS, Thalamati D, Mironescu M, Luo Q, Chai Y, Long Q. New Strategy of Neurodegenerative Disease Treatment with Extracellular Vesicles (EVs) Derived from Mesenchymal Stem Cells (MSCs). *Theranostics*. 2023; 13(12):4138-4165. doi:10.7150/thno.83066.
[73] Palanisamy CP, Phaniendra A, Jayaraman S, Poompradub S. *Nigella sativa* L. seed extracts promotes wound healing progress by activating VEGF and PDGF signalling pathways: *An in vitro* and *in silico* study. *F1000 Research*. 2023; 12: 436.